Paper ID ICLASS06-075

THE EFFECT OF FUEL PROPERTIES ON LIQUID BREAKUP AND ATOMISATION IN GDI SPRAYS

G.Wigley [1], M.Mehdi [1] M.Williams [1] G.Pitcher [2] and J. Helie [3]

[1]Loughborough University, LE11 3TU, UK, g.wigley @lboro.ac.uk
[2]Lotus Engineering, Norwich, NR14 8EZ, UK, gpitcher@lotuscars.co.uk
[3]Siemens VDO, 31036 Toulouse, France, jerome.helie@siemens.com

ABSTRACT Mie imaging and the Phase Doppler technique have been used to determine the spray cone morphology and droplet dynamics of the sprays generated by a GDI pressure swirl injector fuelled with six different liquids, gasoline, n-heptane, E25 a blend of 75% gasoline and 25% ethanol, iso-octane, Exxsol, and Stoddard. Spray cone angle and penetration are inversely linked, with gasoline and n-heptane behaving equally with the smallest cone angles and highest penetration rates. The spray dynamics show distinctly that the development of the spray cone for the other fuels is retarded. Iso-octane and E25 have similar spray characteristics yet widely different fuel properties. Exxsol and Stoddard cannot be recommend for scientific purposes.

Keywords: GDI, PDA, Alternative Fuels, Fuel Properties, Droplet Dynamics, Spray Morphology

1. INTRODUCTION

During the development and production of gasoline fuel injectors standard fuels are used, rather than gasoline, to assess their performance. Furthermore, within the research community, idealised fuels are used where the chemistry is simplified and well documented. This is particularly so with fuel spray studies in order to improve safety [1], or to utilise Laser Induced Fluorescence [2]. However, the use of single component fuels can have a pronounced effect on the spray development in engine like conditions [3].

The effect of fuel type on the liquid breakup and atomization is to be detailed for a modern pressure swirl gasoline direct injection system operating at 100 bar line pressure and an injection duration of 1.0 ms. Six different fuels will be used, 95 RON gasoline, test fuels Exxsol D40 and Stoddard, single component fuels, N-heptane and iso-octane and E25, a blend of 75% gasoline with 25% ethanol. Representative properties are presented in Table 1.

Table 1 Representative Fuel Properties

Fuel	Density Kg/m^3	Kinematic Viscosity mm^2/s	Surface tension mN/m
Gasoline	745	0.74	21.0
N-heptane	682	0.60	20.14
Iso-octane	690	0.72	18.77
E25	755	0.94	22.0
Exxsol	772	1.30	24.7
Stoddard	780	1.28	26.0

Mie imaging will be used to capture the morphology of the spray cone and the Phase Doppler technique, PDA, will be used map out the downstream droplet flow field under atmospheric conditions for each fuel. Radial profiles of the axial and radial velocities and dropsize will be presented at 40 mm below the nozzle tip.

2.1 INJECTOR AND SPRAY RIG

The pressure swirl GDI injector was supported from a gantry incorporating a rotation stage and three precision orthogonal linear traverses to position the spray in three dimensions relative to the static PDA measurement volume. The measurement co-ordinates in the vertical plane were Z = 10, 20, 40 and 80 mm below the nozzle tip. Each radial scan started from the geometric vertical axis through the nozzle tip and traversed out to the periphery of the spray. This horizontal traverse was computer controlled and programmed with a minimum radial step increment of 0.5, 1.0, 2.0 and 4.0 at Z = 10, 20, 40 and 80 mm respectively in order to resolve local high velocity gradients across the cone of the spray in each horizontal plane.

The injector was fuelled, in turn, with 95 RON unleaded gasoline, N-heptane, iso-octane, Exxsol, Stoddard and E25, a blend of 75% gasoline and 25% ethanol. The fuel line pressure was 100 bar pressure. The injection pulse duration time was 2 ms comprising of 1ms soak time and 1 ms fuel delivery.

2.2 PDA AND IMAGING SYSTEM

For the imaging study a Xenon flash unit was the light source. This was coupled to a fibre optic panel to provide a uniform background light intensity distribution against which the nozzle and spray was imaged. The light flash was approximately 8 μs long, however, the flash timing corresponding to maximum intensity was used as the trigger to activate the camera with its exposure time set to 0.5 μs. The main aim of the imaging work was to quantify the spray cone angle and its penetration.

Single-shot images were digitally recorded with a PCO Sensicam Fast Shutter CCD camera equipped with a Nikon 55 mm focal length macro lens. The focus for the lens was the vertical plane through the injector axis. The camera provided an image size of approximately 50 by 40 mm, represented by 1280 by 1024 pixels.

The injector control unit provided electronic triggers, referenced to the opening pulse of the injector solenoid, which, through a variable delay unit, controlled both the flash and image capture time. The time delay between consecutive images was set at 80 μs .Twenty images were stored for each incremental time delay to allow, (1) an evaluation of shot to shot variations and (2) a mean image to be created to highlight bulk features of the spray cone.

The design, construction and application of the two component PDA transmission system to GDI fuel sprays has been well documented [4]. The configuration for the 488 and 514 nm laser beam wavelengths at the final focussing lens was:- beam diameters of 5 mm, equal beam pair separations of 50 mm, laser powers of 100 and 200 milli-watts per beam, and, with a focal length lens of 300 mm produced coincident measurement volumes of diameters of 56 and 59 microns with fringe spacings of 3.10 and 2.94 microns respectively for the two wavelengths. This produced an experimental velocity bandwidth of nominally -30 to 110 m/s.

The standard Dantec 57X10 receiver optical system was positioned at a scattering angle of 70 degrees with the aperture micrometer setting set to 0.5 mm. This optical configuration resulted in an effective measurement volume length of 0.1 mm and a maximum drop size measurement range of up to 100 microns.

At each measurement position 30,000 validated data samples were attempted or an elapsed time of 200 seconds was reached i.e. 1000 injections. The outer radial limit of the spray was defined as the next position after which 'time out' occurred.

3. RESULTS AND DISCUSSION

The spray cone angle and penetration were derived from the mean of 20 images obtained at the instant that the injector was programmed to close as this represented the full development of the cone. The spray boundary was quantified as the 50% image intensity threshold by using colour coded stepped intensity contours. The mean image obtained for gasoline is shown in Figure 1.

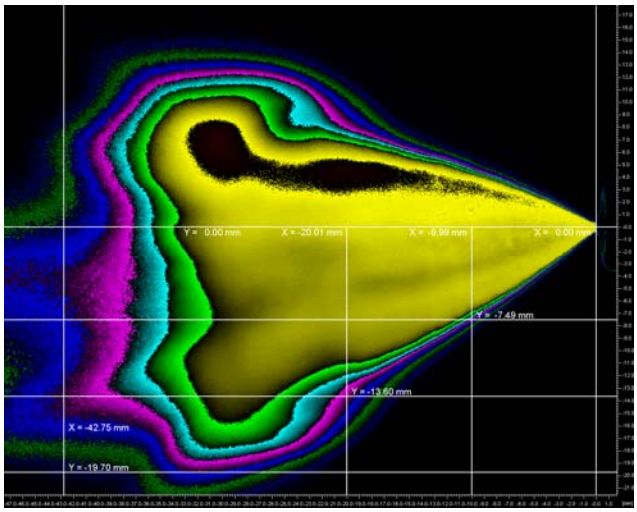

Fig. 1 Mean Image for Gasoline

The spray is asymmetric about the axis through the injector, Y = 0 mm, as the nozzle was configured to give a 'bent angle' of nominally 7.5^0 for targeting purposes. Two estimates of the semi spray cone angle relative to the injector axis are given corresponding to Z = 10 and 20 mm in Table 2. The axial and radial penetration of the spray boundary relative to the injector axis is plotted in Figure 2.

Table 2 Fuel Spray Semi Cone Angles

Fuel	Semi Cone Angle Z = 10 mm	Semi Cone Angle Z = 20 mm
Gasoline	36.83^0	34.22^0
N-heptane	36.91^0	33.98^0
Iso_Octane	37.92^0	36.22^0
E25	37.23^0	35.85^0
Exssol	37.52^0	34.49^0
Stoddard	38.76^0	38.10^0

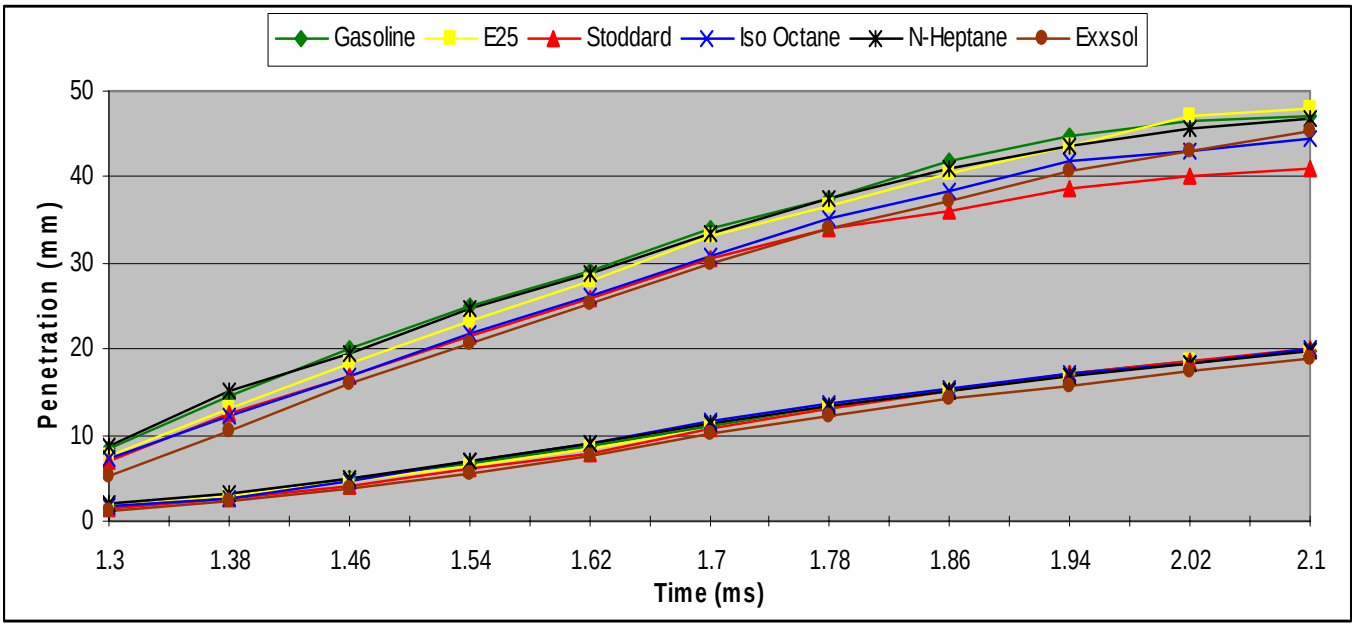

Fig. 2 Axial and Radial Penetration Profiles

For the near nozzle location, Z = 10 mm, gasoline exhibits the smallest cone angle, 36.83^0 , with Stoddard, the largest at 38.76^0. The dominant physical process occurring in the spray here is break up of the liquid sheet immediately downstream from the nozzle exit.

The spray cone angles are smaller for the 20 mm location and have a greater variation of 4^0. There is a shear induced entrainment into the spray cone boundary which reduces the cone angle and, as the atomization of the liquid fuel progresses differently for each fuel, larger variations in the cone angle here can be expected.

There is a definite inverse correlation between the spray cone angle at Z = 10 mm and the axial penetration of the spray cone boundary as seen in Figure 2. Gasoline and N-heptane have virtually equal low cone angles and high penetration rates while Stoddard has the largest cone angle and lowest axial penetration. It might be considered that the axial momentum accounts for this and the controlling fluid parameter would be the liquid density but this is not the case, especially since iso-octane, 690 Kg/m^3 has a similar cone angle and axial penetration as Exxsol with a density of 770 Kg/m^3. Penetration should also be higher for those fuels with lower viscosities. However, this would not explain why E25 penetrates faster than iso-octane. Variations in fluid properties have little influence on the radial penetration, this is virtually identical for the fuels studied so it is purely a function of nozzle geometry.

The determination of spray characteristics from spray images only yields information as regards the spray boundary, the spray morphology. With small differences to be expected between the sprays with the different fuels the emphasis must be put on the spray dynamics as obtained by the PDA technique.

In presenting the PDA data the paper focusses on data at Z = 40 mm where the spray dynamics can be wholly attributed to the atomized fuel. The raw PDA droplet data were time bin averaged into consecutive sectors of 40 μm to provide time varying mean axial and radial droplet velocities and droplet size profiles.

Since the intention is to quantify the differences between the fuels the emphasis is really on experimental consistency. The optical and electronic system parameters were adjusted for high gain for small droplet detection and to minimize the effect of laser beam obscuration by the spray while ensuring rejection of opto-electronic noise. The system parameters were then fixed throughout the measurement programme. Before each measurement scan was made across a spray radius, the alignment of the optical system with the injector nozzle was confirmed.

The largest contributor to fluctuations in the estimates of droplet velocity and size is the number of samples collected in any one time bin. As the sprays are highly transient small time bins had to be chosen and the sample number in any time bin is related to the measurement location. As an indicator to the statistical significance of the data presented in this paper a plot of the sample number in the time bin representing maximum axial droplet velocity for gasoline is shown in Figure 3. The sample number between the axis through the injector, R = 0 mm and R = 12 mm is low, the smallest counts are between 10 and 20 samples at R = 8 mm. However, as long as the velocity and dropsize variation are small inside the hollow cone then significant estimates can still be expected. Obscuration of the input laser beams is the primary cause for low data counts, particularly on the inside surface of the spray cone, i.e. R = 12 to 18 mm.

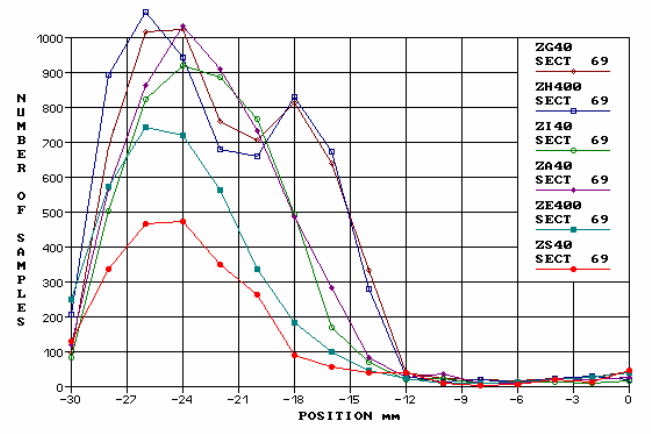

Fig. 3 PDA sample number distributions in sector 69

Nevertheless, the number counts here are sufficiently high and the velocity and dropsize estimates should have a good statistical significance. Although these distributions cannot be used to quantify droplet density between the fuels they do serve as an indicator of the variation in atomization quality, i.e. high sample counts. N-heptane, file ZH40, demonstrates a high level of atomization especially on the inside of the spray cone. Gasoline, ZG40,, iso-octane, ZI40, and E25, ZA40, all show similar atomization characteristics. Exxsol, ZE40, and Stoddard, ZS40, are widely different with their high values of viscosity and surface tension.

The mean droplet axial velocity profiles across the spray radius at Z = 40 mm are shown for each fuel in Figure 4. The cross-section for the measurement scan was the same as that used for estimates of the spray cone angle and penetration.

The time dependence is given by the sector number. With each sector being 40 μs then sectors 60 to 72 represent the time total period 2.36 to 2.88 ms. The time span corresponds to the development of the spray cone 40 mm below the nozzle.

These times refer to the time after the start of the electronic pulse of 2 ms which included a soak time of 1 ms. This soak time improves the time response of the injector but there is a corresponding shift in time for the needle to open and for the actual fuel delivery to begin.

Apart from the industry test fuels, Exxsol and Stoddard, the general trend for the axial velocity profiles for the developing spray cones is for a peak, at approximately 30 m/s, to occur in the velocity profiles at a nominal radius of R = 18 mm at sector 60, i.e. 2.36 to 2.40 ms. As time increases the peak velocity increases, up to 54 m/s, and its location moves inboard, towards R = 14 mm.

As with the spray morphology data there are distinct similarities between the data for Gasoline and N-heptane and the data for iso-octane and E25. The high axial penetration of Gasoline and N-heptane is confirmed with the highest recorded axial velocities of 54 m/s. However, between sectors 60 and 66 N-heptane demonstrates higher peak velocities and sample numbers, suggesting better atomization due to low density, viscosity and surface tension.

The PDA data also show that during the early cone development the iso-octane spray cone develops faster than the E25 spray but between sectors 69 and 72 they are identical. However, this does not conform to the trend expected from the axial penetration data which shows E25 penetrating faster.

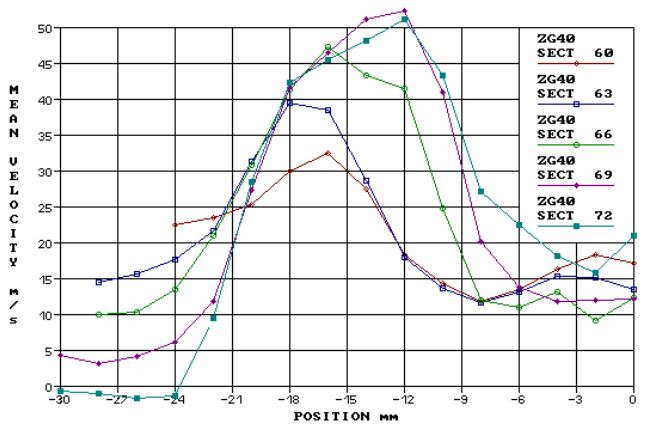

Gasoline

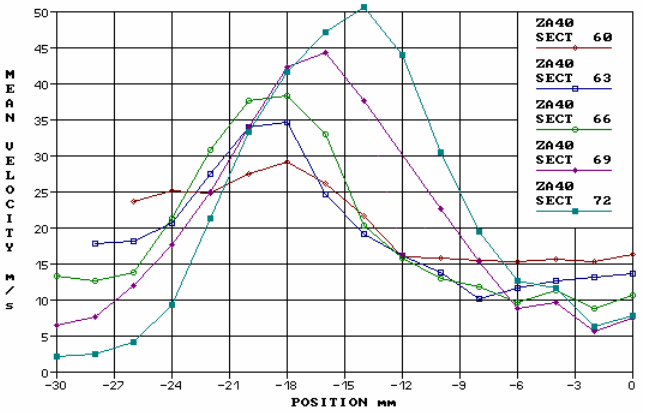

E25

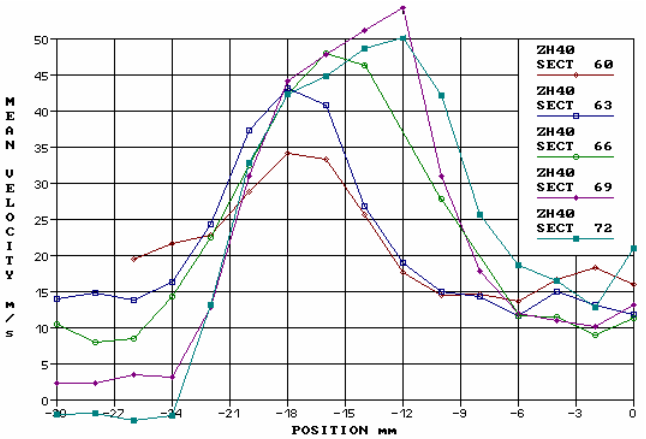

N-heptane

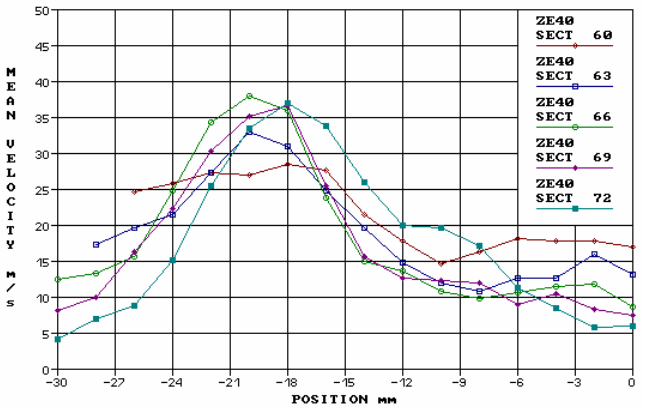

Exxsol

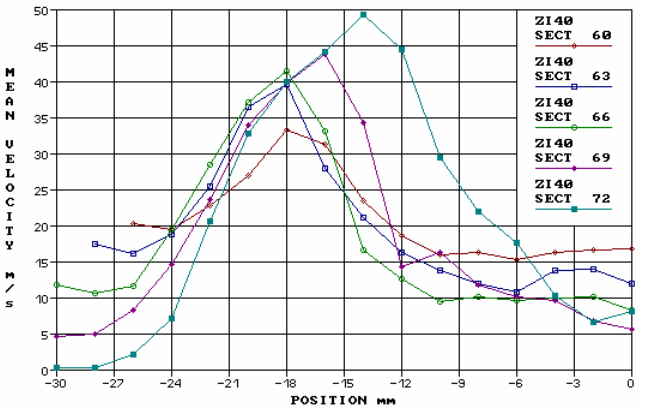

Iso-Octane

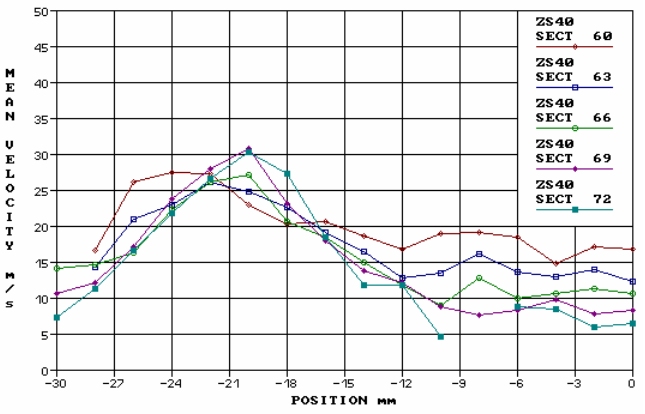

Stoddard

Fig. 4 Axial Velocity Profiles 40 mm below the nozzle

These four fuels demonstrate a very similar behaviour in the spray periphery, R > 24 mm, with the axial velocities decaying from approximately 20 m/s at sector 60, down to near zero flow at sector 72. The axial velocity profiles are remarkably smooth inside the 'hollow cone' of the spray considering how few samples make up the velocity estimates but do show variation of up to 10 m/s as a function of time.

The poor axial penetration of the Exxsol and Stoddard sprays is due to the much lower droplet velocities, less than 40 m/s for Exxsol and only 30 m/s for Stoddard. Furthermore, the variation in axial velocity is small, less than 10 m/s, and the radial position of the peak velocity can be found between 18 and 20 mm for the whole duration of the spray cone development.

Whereas these velocity profiles are essential for quantifying small differences between the sprays they do not necessarily provide an intuitive picture of the spray dynamics. Rather than perform a similar analysis for the radial velocity profiles the two velocity components have been combined to allow a presentation of the droplet vector flow field. Two time sectors have been chosen, that representing the maximum axial velocity, i.e. a time of 2.74 ms and the time at which the spray cone starts to collapse with the end of injection, a time of 2.98 ms. These vector flow maps are shown in Figures 5 and 6 respectively with the axis through the injector in the middle and with the vertical lines either side at R = 10, 20 and 30 mm. The vectors have a constant 2 mm spacing along the radius.

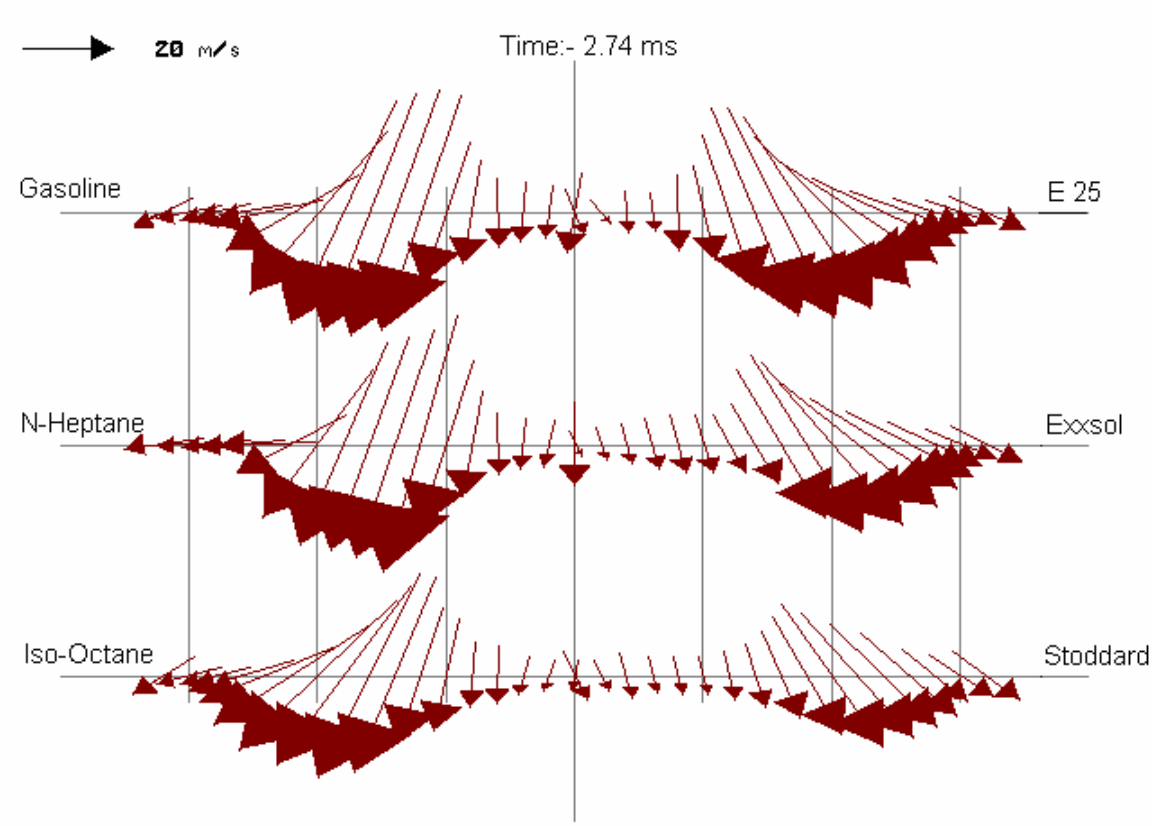

Fig. 5 Flow field map at Z = 40 mm and Time 2.74 ms for all fuels

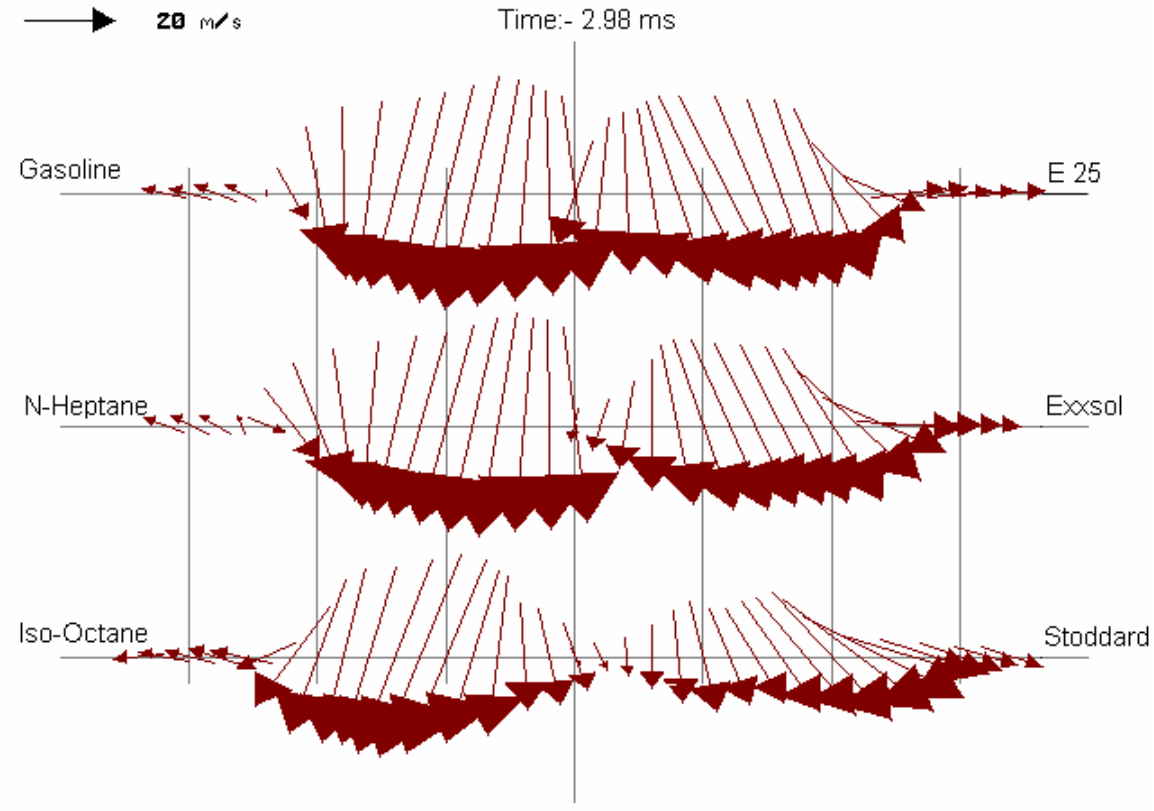

Fig. 6 Flow field map at Z = 40 mm and Time 2.98 ms for all fuels

The flow angle and the velocity distribution across the spray cone are now readily visualized. The key to understanding the spray development lies with the magnitude of the vectors, the generation of the vortex, or recirculation zone, due to entrainment into the spray periphery and the transition of the spray towards the injector axis as the spray cone collapses.

The gasoline and N-heptane sprays have identical flow angles across the centre of the spray cone but the latter appears to be to be in advance of the gasoline spray as the flow vectors from 22 mm outwards are already turning into the vortex with a zero axial flow component.

The isoctane spray has much reduced flow vector magnitudes across the cone when compared to the above, but, since the radial flow components are similar to gasoline the effect is to produce a steeper flow angle although the vortex still has to form. These comments apply equally to the flow field for E25.

It is again obvious that Exxsol and Stoddard produce widely different flow fields to the other fuels. Since the axial flow component has reduced in comparison to the radial flow component the flow vectors are at steeper angles across the spray cone yet, with the reduced entrainment, the vortex has yet to appear.

At the later time of 2.98 ms the vortex on the spray periphery is clearly seen in the case of N-heptane and gasoline while for iso-octane the vortex has only just formed. For E25 and Exxsol the axial flow component in the spray periphery has decayed to zero but for Stoddard the lag is appreciable as there is still no vortex appearing.

The largest difference between the fuels is seen in the manner that the sprays for gasoline and N-heptane tend to produce a full cone spray as the maximum vectors occur close to the injector axis. E25 is the only other fuel that is beginning to demonstrate this behaviour. The spray cone is still in evidence for iso-octane, Exxsol and Stoddard.

To reinforce the differences between the fuels at this time the axial and radial droplet velocity and dropsize profiles are shown in Figure 7. The key to the profiles for each fuel is given in the top figure, where the file names, from top to bottom, refer to; gasoline, N-heptane, iso-octane, E25, Exxsol and Stoddard respectively.

The peak in the axial velocity profile for gasoline and N-heptane occurs at R = 8 and 7 mm respectively. As the full spray cone is bent, at an angle of nominally 7.5^0 to the injector axis, the expected offset for symmetry would be 5 mm. Furthermore, the sample distributions show a dramatic increase in sample count in the centre of the spray. To all intents and purposes these fuels produce a full cone spray after the collapse of the spray cone in the far field region downstream from the nozzle. The similarity between these two fuels is also seen in the radial velocity components where negative flows occur during the high shear of the axial profiles at R = 22 mm which correlates to the smallest dropsizes recorded, less than 2 microns. The dropsize value here is the arithmetic mean, D_{10}.

Inboard from the minima in the dropsize profiles there is a step change in the slope of the profile. This corresponds to the collapse of the inside surface of the spray cone. In this region N-heptane produces the smallest droplets, from 5 to 7 μm followed by E25 and gasoline.

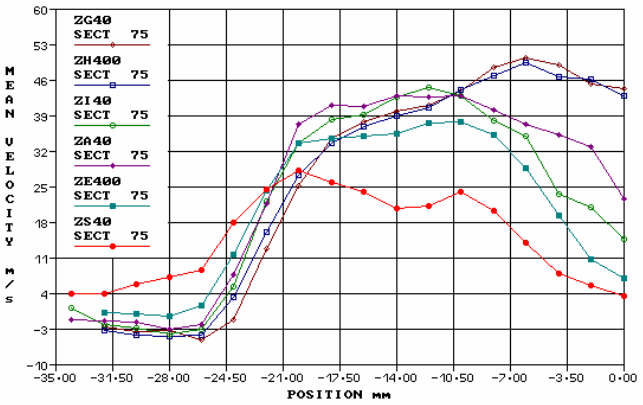

Axial Velocity

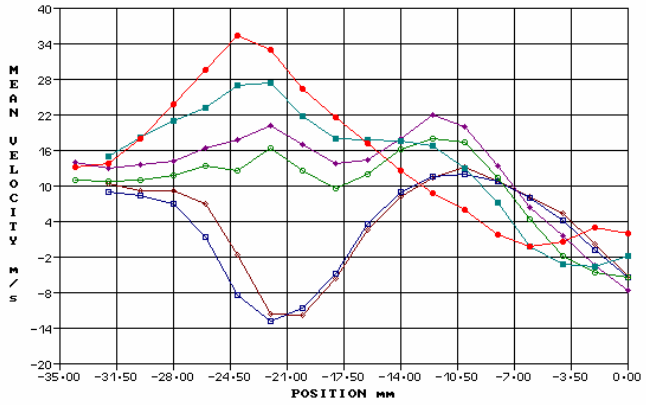

Radial Velocity

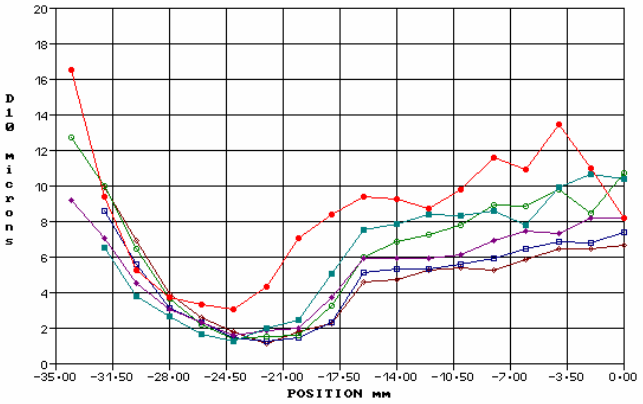

Dropsize

Fig. 7 Velocity and dropsize profiles at Z = 40 mm and time 2.98 ms.

The droplets in the iso-octane and Exxsol sprays are some 2 to 3 μm larger whereas, for Stoddard, the dropsize is double with up to 10 μm diameter. However, the scatter is large indicating a small sample number, but no less than 50, and a wide range in individual dropsizes.

The dropsizes in the spray periphery, R > 28 mm increase dramatically from less than 4 μm to approach 20 μm. The axial velocity component for these droplets is virtually zero with a radial velocity component of between 10 and 15 m/s. Although Stoddard produces the largest dropsizes it is also the slowest penetrating of the fuels.

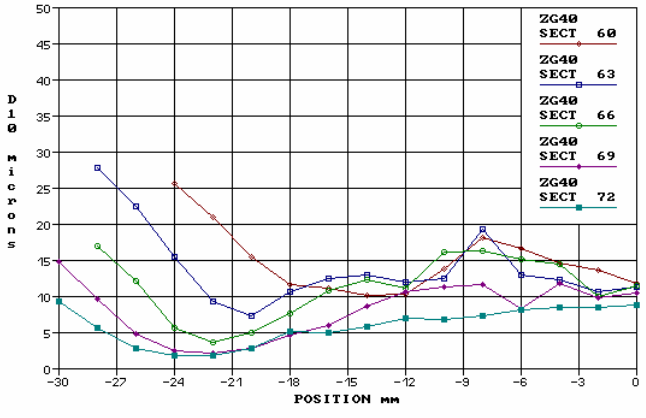

Gasoline

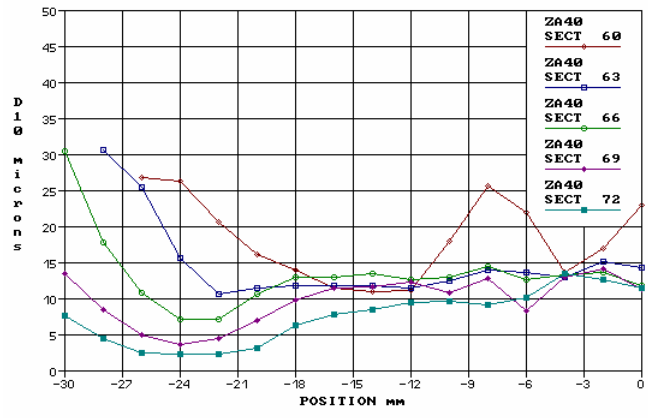

E25

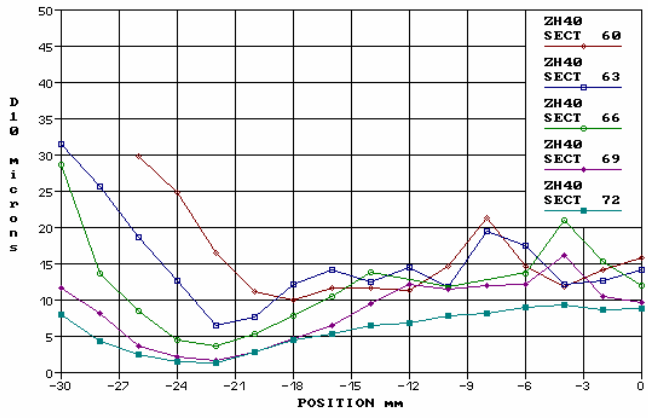

N-heptane

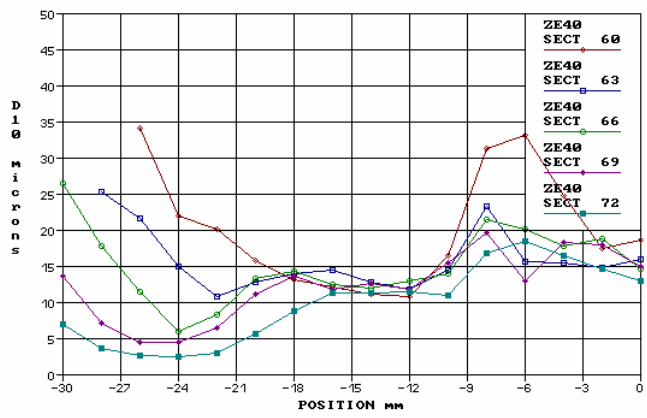

Exxsol

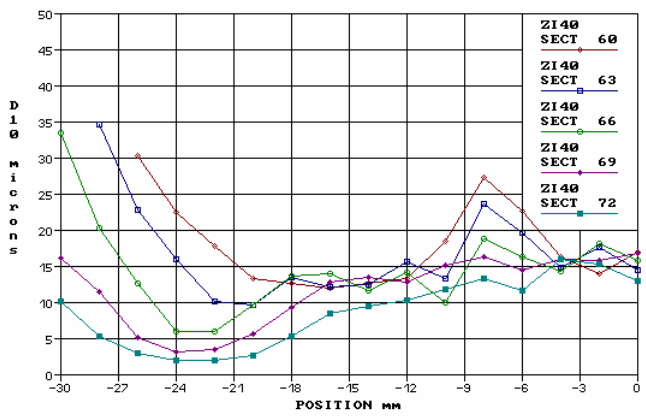

Iso-Octane

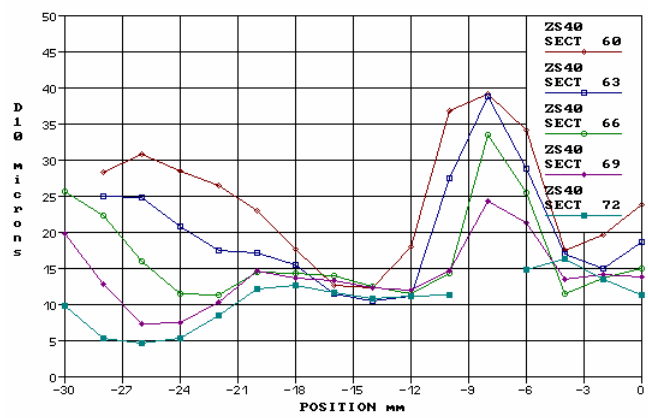

Stoddard

Fig. 8 Dropsize Profiles 40 mm below the nozzle

The discussion above considered the dropsizes for the fuels at the time of spray cone collapse. This part now considers the dropsize profiles during the development of the spray cone. This figure complements Figure 4 which shows the axial velocity profiles 40 mm below the nozzle.

In comparing the temporal variation in dropsizes with time for the fuels it is convenient to divide the plots into three spatial domains, R = 0 to 12 mm, 12 to 18 mm and 18 to 30 mm. The latter refers to the spray periphery and the high shear gradient of the axial velocity profiles. All fuels produce similar droplet size profiles with a consistent decay in size with increasing time.

In the region of the highest droplet velocities, R = 12 to 18 mm there is a similar decrease in dropsize with time except for the early cone in sector 60. The high velocities also lead to a small variation in size particularly for the fuels that have low penetration rates, Stoddard, Exxsol and iso-octane.

By far the largest variation in dropsizes between the fuels can be found between the injector axis and the inside surface of the spray cone. Again, the dropsize profiles decay with time for each fuel, but, apart from gasoline each profile exhibits a definite peak centered about R = 8 mm. The less penetrating the fuel spray the greater the

peak dropsize. Over these time sectors this region sees the transition from the pre-swirl component of the spray to the growth of the spray cone. Large mean dropsizes here are a consequence of poor penetration and atomization in the pre-swirl spray which results in a wide dropsize range with few small droplets.

To conclude the discussion of droplet size distributions the dropsize profiles for the six fuels are shown in Figure 9 for sector 69, the time of 2.74 ms when the peak axial droplet velocities are seen in the plane 40 mm downstream from the nozzle. A family of curves is evident with a radial shift outwards in the minima as dropsizes for each fuel increase. The minimum is located at the base of the axial shear velocity gradient. The step changes in the dropsize profiles, between R = 12 and 20 mm for gasoline and Stoddard respectively, occurs at the location of the maximum axial velocity.

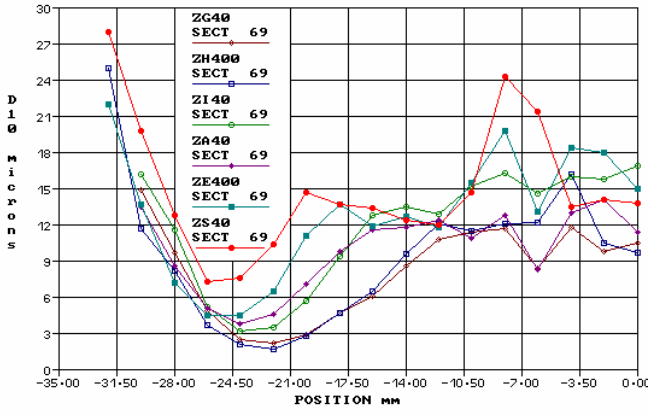

Fig. 9 Dropsize profiles at Z = 40 mm and time 2.74 ms.

4. CONCLUSIONS

Mie imaging and the Phase Doppler technique have been used to determine the spray morphology and dynamics of the sprays produced by a pressure swirl GDI injector when operated with six different fuels. The need for using these fuels stems from scientific requirements to either model gasoline with a single component fuel or for safety reasons while in industry stable and well defined fuels are needed for injection calibration.

Basically N-heptane can be used to model gasoline as regards spray morphology and droplet dynamics. The same is true for iso-octane to model E25. However, for scientific purposes it would be difficult to relate data from Exxsol and Stoddard to describe a gasoline spray.

Compared with gasoline and n-heptane the other fuels produce lower axial penetration rates and higher spray cone angles. The radial penetration rates are not particularly sensitive to fuel type. The spray dynamics show that the spray cone development is essentially retarded. The axial velocities are reduced which leads to a decrease in the shear gradient, a reduction in entrainment and an increase dropsizes. The consequences of this are the very late development of, firstly, the vortex just upstream from the leading edge of the spray cone and, secondly, production of a full cone spray after the spray cone collapses.

In general fuels with higher density, viscosity and surface tension than gasoline exhibit this retarded development. However, it is not known why iso-octane models E25 so well as their physical properties are quite different. The bulk properties for E25 have been calculated as a simple ratio of the gasoline and ethanol components. However, since there is a migration of the species with the lowest surface tension to the interface it is the interfacial properties that are required for the blend [5].

5. ACKNOWLEDGEMENTS

Support from Inov8, Buckingham, UK for the supply of the industrial test fuels and their physical properties data.

6. REFERENCES

1. K.H. Lee, C.H. Lee and C.S. Lee, Analysis of size-classified spray structure and atomization mechanism for a gasoline direct injector, Atomization and Sprays, Vol. 14, pp.545 – 562, 2004.
2. C. Shulz and V. Sick, ‘Tracer-LIF Diagnostics: Quantitative Measurement of fuel concentration, temperature and fuel/air ratio in practical combustion systems’ Prog. Energy Combustion Science 31, 75-121, 2005.
3. M.C. Drake, T.D. Fansler, A.S. Solomon and G.A. Szekely Jr., ‘Piston fuel films as a source of smoke and hydrocarbon emissions from a wall controlled spark ignited direction-injection engine’, SAE 2003-01-0547, 2003.
4. G. Wigley, G. Hargrave and J. Heath, ‘A High Power, High Resolution LDA/PDA System Applied to Gasoline Direct Injection Sprays’, Particle & Particle Systems Characterization, Vol. 1, 1999.
5. J. Escobedo and G.A. Mansoori, Surface Tension Prediction for Liquid Mixtures, AIChE, vol. 44, pp 2324-2332,1998.